CROSS-SHORE SAND TRANSPORT AND BED COMPOSITION

Leo C. van Rijn[1]

1. INTRODUCTION

The sediment bed of the coastal zone usually exhibits a large variation of sediment sizes. Local variations related to the presence of bed forms (differences in size at the top and in the trough) may occur, but cross-shore sorting due to selective transport processes is a more important process in nature (fining in seaward direction). These effects can only be represented by taking the full size composition of the bed material, which may vary across the profile, into account.

2. DESCRIPTION OF MODELS

2.1 Wave propagation and longshore currents

The propagation and transformation of individual waves (wave by wave approach) is described by a probabilistic model (Van Rijn and Wijnberg, 1996). The individual waves shoal until an empirical criterion for breaking is satisfied. Wave height decay after breaking is modelled by using an energy dissipation method. Wave-induced set-up and set-down and breaking-associated longshore currents are also modelled. The near-bed orbital velocities of the high-frequency waves (low-frequency effects are neglected) are described by second order Stokes theory and by linear wave theory in combination with an empirical correction factor. The depth-averaged return current (u_r) under the wave trough of each individual wave (summation over wave classes) is derived from linear mass transport and the water depth (h_t) under the trough. Streaming in the wave boundary layer due to viscous and turbulent diffusion of fluid momentum is taken into account. The streaming (u_b) in the wave boundary layer is of the order of 5% of the orbital peak velocity and generally onshore-directed in deeper water (symmetric waves). In shoaling waves in shallow water, the streaming in the boundary layer may be offshore-directed.

2.2. Sand transport; single fraction method (SF-method)

The sand transport rate for each wave (or wave class) is based on the computed wave

---

[1] Delft Hydraulics and Dep. of Phys. Geography, Univ. of Utrecht, P.O. Box 177, 2600MH, Delft, The Netherlands

height, depth-averaged cross-shore and longshore velocities, orbital velocities, friction factors and sediment parameters..

The net (averaged over the wave period) total sediment transport is obtained as the sum of net the bed load (q_b) and net suspended load (q_s) transport rates.

The net bed-load transport rate is obtained by time-averaging (over the wave period) of the instantaneous transport rate using a formula-type of approach.

The net suspended load transport is obtained as the sum ($q_s = q_{s,c} + q_{s,w}$) of the net current-related and the wave-related transport components (see, Van Rijn, 1993). The current-related suspended load transport ($q_{s,c}$) is defined as the transport of sediment particles by the time-averaged (mean) current velocities (longshore currents, rip currents, undertow currents). The wave-related suspended sediment transport ($q_{s,w}$) is defined as the transport of sediment particles by the oscillating fluid components (cross-shore orbital motion). The $q_{s,w}$-component includes a calibration coefficient γ in the range between 0.3 and 0.7. Computation of the wave-related and current-related suspended load transport components requires information of the time-averaged current velocity profile and sediment concentration profile.

The current velocity profile is represented as a two-layer system to account for the wave effects in the near-bed layer (Van Rijn and Kroon, 1992; Van Rijn, 1993). The convection-diffusion equation is applied to compute the equilibrium time-averaged sediment concentration profile for current-related and wave-related mixing. The effect of the local cross-shore bed slope on the transport rate is taken into account (see Van Rijn, 1993). Details are given by Van Rijn and Kroon (1992); Van Rijn (1993, 1997).

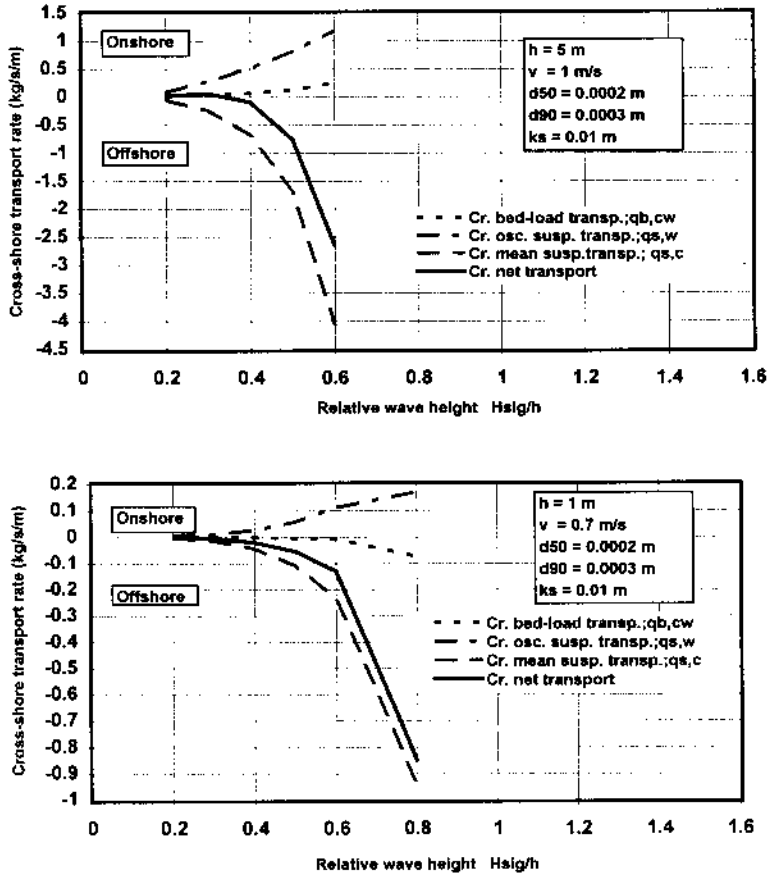

Figure 1 *Cross-shore transport components as a function of relative wave height*

To get a better understanding of the relative importance of the three cross-shore transport components $q_{b,cw}$ =mean and oscillating bed-load transport , $q_{s,w}$ = oscillating suspended transport (only high-frequency) and $q_{s,c}$ = mean suspended transport; some sensitivity computations using the single wave method and the single fraction method have been made for two water depths. The γ-factor of the $q_{s,w}$ transport component is taken as 0.3 to obtain values of the right order of magnitude compared to measured data (Kroon, 1994; Houwman and Ruessink, 1996 and Wolf, 1997). The computations have been made for uniform water depths of 1 and 5 m. The wave period is 7 s. The waves are normal to the coast. The longshore (tide- or wind-driven) depth-averaged current velocities are taken as 0.7 and 1 m/s. The bed roughness is $k_{s,c}=k_{s,w}=0.01$ m for all conditions. The water temperature is 15 ^{o}C, the salinity is 30 promille.

Figure 1 shows computed values of the three cross-shore transport components and the net transport as a function of relative wave height H_s/h for bed material of 200 μm. For a depth of 5 m the net total transport is offshore-directed for $H_s/h > 0.3$. For a depth of 1 m the net total transport is offshore-directed for all conditions. Since, the net total transport in cross-shore direction is a delicate balance of all cross-shore transport components involved, the γ-factor of the osc. suspended transport has a great influence on the net transport. Additional calibration of the γ-factor remains necessary. Furthermore, also the low-frequency transport component (neglected in this study) may have some effect on the cross-shore transport balance.

2.3 Multi-fraction method (MF-method)

Generally, the approach is to divide the bed material in a number of size fractions and to compute the sand transport rate of each size fraction using an existing single fraction method (replacing the median diameter of the bed material by the mean diameter of each fraction) with a correction factor (ξ_i) to account for the non-uniformity effects. Herein, the correction factor of Egiazaroff (1965) is used. The total sand transport rate for all size fractions can be obtained by summation of the transport rates per fraction taking the probability of occurrence of each size fraction into account. The multi-fraction method incorporates two effects:

- transport is non-linearly dependent on particle diameter, for example: suspended load transport is inversely proportional to size; $q_s \approx d^m$ with m between -0.5 and -2,
- hiding effect of smaller particles between the larger particles.

The influence of the hiding factor is a reduction of the transport rate in the case of dominant suspended load transport, because the critical bed-shear stress of the finer particles (hiding between the coarser particles) is enlarged.

2.4 Bed Level changes and sediment composition

Bed level changes per fraction i are described by:

$$\rho_s(1-e)\partial z_{b,i}/\partial t + \partial(p_i q_{t,i})/\partial x = 0 \qquad (1)$$

with: z_b= bed level to datum, $q_{t,i}= q_{b,i} + q_{s,i}$= volumetric total load (bed load plus suspended load) transport per fraction i, p_i= value of fraction i, ρ_s= sediment density, e= porosity factor.

The total bed level change is obtained by summation of fractional bed level changes over all N-fractions: $\Delta z_{b,x,t} = \Sigma \Delta z_{b,i,x,t}$

The bed material is computed in a thin (order of 0.1 m) surface mixing layer of thickness δ applying a one-layer approach. This approach was introduced by Hirano (1971) and later extended by Ribberink (1987). The thickness of the surface layer is herein assumed to be constant in space and time and is moving in vertical direction with the bed surface in response to bed level changes (deposition upwards and erosion downwards). Thus, the surface layer is always at the top of the bed. The mixing of sediment within the surface layer is assumed to be effectuated within each time step (instantaneous mixing) through small-scale bed form migration processes in the lower regime or by wave-induced vortices in the sheet flow regime.

At present stage of research the bed material composition of the subsoil below the surface layer is assumed to be uniform (no layered structure) and equal to the initially specified fraction values ($p_{0,i,x}$).

The bed material composition is computed according to the following procedure:

- the sediment mass M of the surface layer at $t = 0$ is subdivided in masses $M_{x,i}$ based on the initial fraction values $p_{o,x,i}$, as follows: $M_{x,i} = p_{o,x,i}\, M$,
- the sediment mass $M_{x,i}$ of fraction i changes due to sediment deposition or erosion at the surface of the bed; in case of deposition the mixing layer will move upward at a rate equal to the deposition rate, while an equal amount of sediment with the composition of the mixing layer will be lost at the bottom (exchange at base) of the mixing layer; in case of erosion the opposite process will take place and the mixing layer will move downward eroding itself into the subsoil, hence sediment with the composition of the subsoil will be absorbed by the mixing layer;
- the new composition of the bed material is given by: $p_{x,i,t+\Delta t} = M_{x,i,t+\Delta t}/M$

3. SENSITIVITY COMPUTATIONS SAND TRANSPORT

3.1 Effect of single and multi-wave approach on sediment transport in uniform conditions (constant depth)

To analyze the effect of single and multi-wave modelling on the current-related (longshore) sand transport rates, sensitivity computations have been made for a specific case with a constant water depth $h = 3$m. The bed material is represented as single fraction material with $d_{50} = 0.0002$ m and $d_{90} = 0.0003$ m and the bed roughness is taken to be $k_{s,c} = k_{s,w} = 0.01$ m. The irregular waves (normal to the coast) are assumed to have a Rayleigh-distribution with $H_{rms} = 0.71$ m, $H_{1/3} = 1$ m and $T_p = 7$ s. The longshore current velocities have been varied in the range between 0.2 and 2 m/s. The water temperature is taken as 15 ^{o}C and the salinity as 30 promille.

The current-related sand transport rates have been computed in three ways:

- based on a single representative wave height equal to H_{rms},
- based on a single representative wave height equal to $H_{1/3}$,
- based on multi-wave approach, schematizing the Rayleigh-distribution to 8 wave height classes between 0.2 and 1.6 m and wave periods between 6.2 and 7.6 s.

The results are presented in Figure 2, showing the ratio of transport rates based on the single wave approach and the multi-wave approach. Application of $H_{1/3}$ as the representative wave height yields transport rates which are considerably larger than those of the multi-wave approach (factor 2 for low velocities). Application of the H_{rms} leads to transport rates, which are much smaller (factor 2 for low velocities). The discrepancies are relatively large for low current velocities, when the waves are the dominant factor in

the transport process. For high current velocities the proper representation of the wave field becomes less important with respect to the transport process.

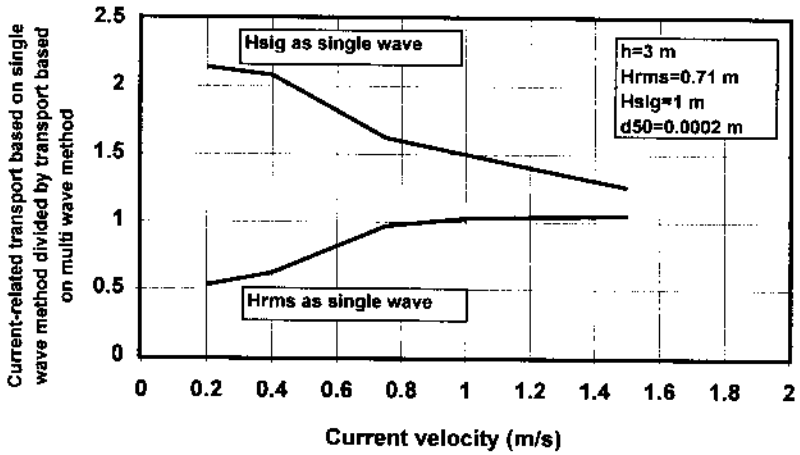

Figure 2 Influence of single and multi-wave approach on sand transport

3.2 Comparison of single and multi-fraction method for sediment transport in uniform conditions (constant depth)

To compare the results of both methods, computations have been made for three types of sediment material (d_{50}=0.2, 0.4 and 0.8 mm) with a symmetrical size distribution using seven fractions (N=7). The water depth was taken as h=3 m. The current velocity was varied in the range of 0.3 to 2 m/s. The wave heights were taken as H_s=0 m and H_s=2 m with a period of T_p=7 s. The angle between the wave and current directions was 90°. The current-related and wave-related bed roughness heights were assumed to be equal and varied in the range of 0.05 to 0.01 m, depending on the hydraulic conditions (smaller values at higher bed-shear stresses). The water temperature was taken to be 15 °C and the salinity 30 promille.

Computation of the suspended load transport using the single fraction method requires information of the size (d_s) of the suspended sediment. Two series of computations have been made for N=1; $d_s=d_{50,bed}$ for all conditions and $d_s=0.7\ d_{50,bed}$ at small bed-shear stresses increasing to $d_s=d_{50,bed}$ at high values of the bed-shear stress.

Figures 3 and 4 show the ratio of the transport rates according to both methods for sediment of 0.2 and 0.4 mm. The bed-load transport includes the wave and current-related transport components; the suspended transport only includes the current-related transport component (wave-related has been neglected).

Bed-load transport ratios ($q_{b,N=1}/q_{b,N=7}$) as well as suspended load transport ratios ($q_{s,N=1}/q_{s,N=7}$) are presented. N=1 refers to the single fraction method; N=7 refers to the multi-fraction method.

Generally, the deviations between the MF and SF-method are largest in the lower transport regime (bed-shear stress slightly greater than critical shear stress) and smallest in the higher transport regime when the bed-shear stress is much larger than the critical bed-shear stress. For all cases (see Figs. 3 and 4) the application of the multi-fraction method results in substantially smaller suspended transport rates, especially at lower velocities. This is caused by the effect of the hiding factor on the reference concentration.

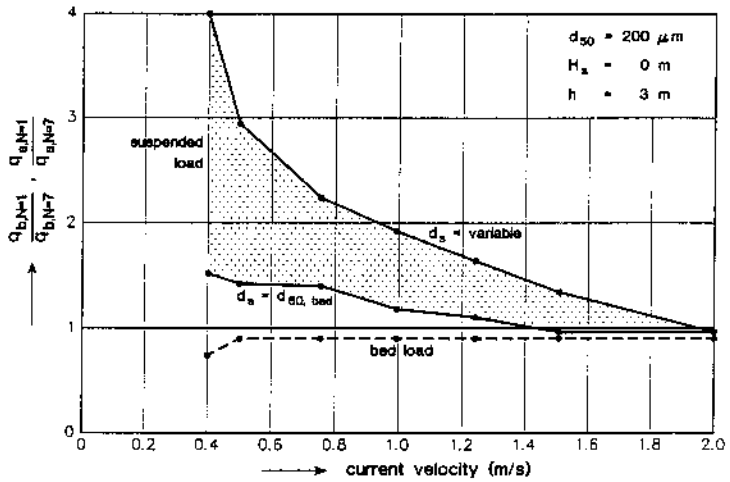

Figure 3 *Ratio of transport rates according to the SF and MF methods (0.2 mm)*

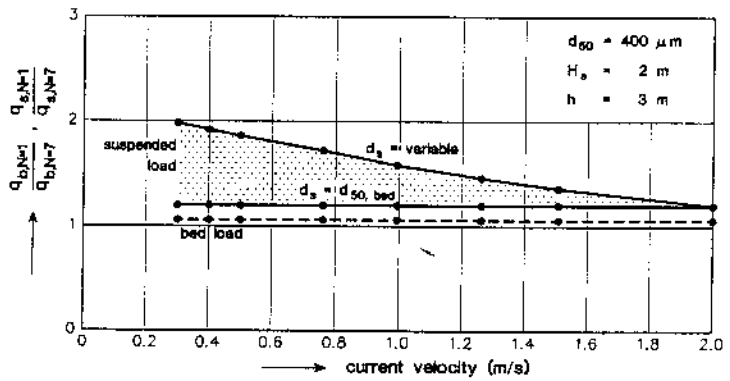

Figure 4 *Ratio of transport rates according to the SF and MF methods (0.4 mm)*

3.3 Comparison of sand transport rates across the surf zone using the single/multi-wave and the single/multi-sand fraction methods

3.3.1 Input data and boundary conditions

Computations have been made for a cross-shore profile of the barrier island coast of Terschelling, The Netherlands (see Van Rijn and Wijnberg, 1996).

Wave conditions: $H_{rms,0}$= 2.8 m T_p= 9 s

Three bed material types: d_{50}= 0.00023 m, d_{50}= 0.0004 m, d_{50}= 0.0008 m

Both the number (N) of sand fractions and the number (NW) of wave height classes have been varied. As regards the sand fractions, N=7 and N=1 have been used. As regards the wave classes, NW=13 (multi-wave approach), NW=5 and NW=1 (single wave approach) have been used. In the latter case the rms-wave height was used as the representative wave height; the wave aproach angle was constant (= 30°) for all NW values. The wave-related suspended transport was not taken into account (γ=0). The longshore velocity (x=0 m) is v_0= 0.7 m/s. Bed roughness is $k_{s,w}$= 0.01 m and $k_{s,c}$= 0.05 m, water temperature Te= 15 degrees C, salinity Sa= 30 promille.

3.3.2 Computed results; influence of number of wave classes (NW=1, 5, 13)

Case 1: storm event $H_{rms,0}$= 2.8 m, d_{50}= 0.00023 m (N=1)
The basic features of the computational results are:

- wave height decreases by bottom friction seaward of the outer bar and by wave breaking at the outer bar to a value of about 2 m; the wave heights are about 15% lower using 13 classes (NW=13) in stead of 1 class (NW=1 based on H_{rms}); the wave heights are within 3% for NW=5 and NW=13 (not shown);
- longshore current is maximum (about 1.8 to 2.4 m/s) just landward of the outer bar; using NW=13 the maximum longshore current is about 30% (1.8 m/s in stead of 2.4 m/s) smaller than for NW=1;for NW=5 and NW=13 the longshore current velocities are within 3% in the bar zone and within 10% near the shoreline;
- offshore current (undertow) is maximum at the crest (about 0.6 m/s); using NW=13 yields smaller (30%) current velocities seaward of the outer bar; for NW=5 and NW=13 the offshore current velocities are within 3% in the bar zone and within 10% near the shoreline;
- the longshore transport rate (sum of bed load and suspended load) shows maximum values just landward of the bar crests (about 10 to 35 kg/s/m) and near the shoreline;
  using NW=1 results in an increase of the longshore transport by a factor 4 compared with the values for NW=13; thus the schematization of the wave spectrum of a storm event has a very pronounced effect on the computed transport; NW=1 (1 wave class) leads to somewhat higher wave heights (5%), but significantly larger longshore current velocities (30%) and hence significantly larger values of the longshore transport rate;
  for NW=5 and NW=13 the longshore transport rates are within 10% in the bar zone and within 30% near the shoreline;
- the cross-shore transport is onshore-directed seaward of the outer bar and in the trough between the bars due to the dominating effect of the bed-load transport, but is offshore-directed in the bar crest zones where the suspended transport is dominant; using NW=1 results in an increase of the cross-shore transport by a factor 4 compared with the values for NW=13, mainly because of an increase of the undertow velocity;
- the cross-shore transport rates in the bar crest zone generally are a factor 10 to 20! smaller than the longshore transport rates;

Computational results for d_{50}= 0.0004 m and d_{50}= 0.0008 m using NW=1 and NW=13 showed similar effects (increase of transport rates at bar crests by factor 4).

3.3.3 Computed results; influence of number of size fractions (multi fraction approach)

Case 1: storm event $H_{rms,0}$= 2.8 m, d_{50}= 0.00023 m
The effects of the number of sediment fractions on the computed longshore and cross-shore total transport rates along the cross-shore profile are presented in Figure 5. The number of wave classes is NW=13.

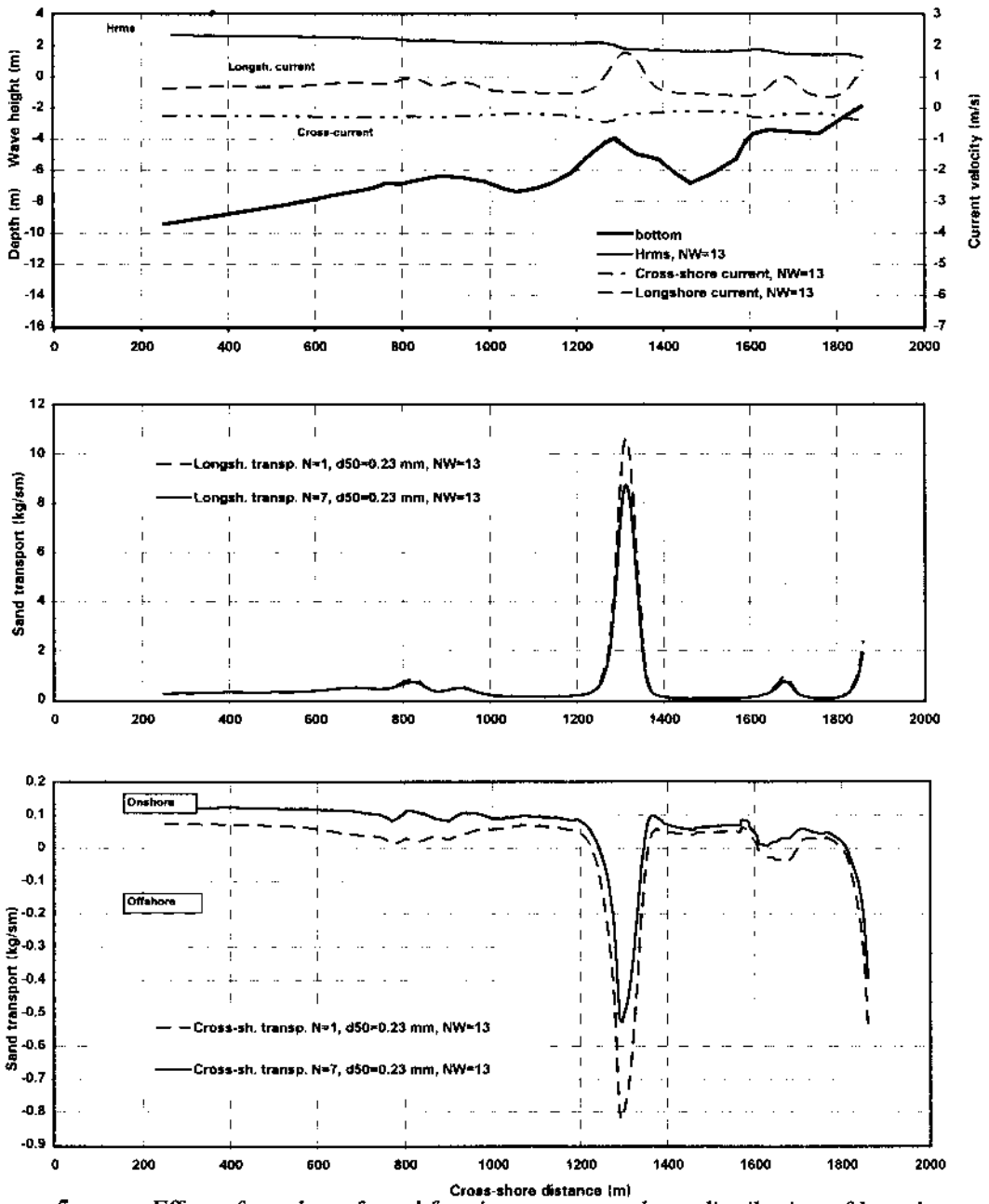

Figure 5 *Effect of number of sand fractions on cross-shore distribution of longshore and cross-shore transport for 230 μm-sediment*

The basic features of the computational results are:

- the longshore transport rate (sum of bed load and suspended load) shows maximum values just landward of the bar crests (about 8 to 10 kg/s/m) and near the shoreline (about 2 kg/s/m);
  the number of sand fractions (N=1 or 7) has little influence on the longshore transport at the crest of the outer bar (10 to 20% difference);
- the cross-shore transport is onshore-directed seaward of the outer bar and in the trough between the bars due to the dominating effect of the bed-load transport, but

is offshore-directed at the bar crest zones where the suspended transport is dominant;

- the cross-shore transport rates in the bar crest zone generally are a factor 10 to 20! smaller than the longshore transport rates;
- the onshore transport seaward of the outer bar shows a large increase (factor 2 to 4) using N=7 sand fractions in stead of N=1; this can be be explained by comparing the data at x=804 m, which are:

N=7	$q_{b,cross}$= 0.204	kg/s/m
	$q_{s,cross}$= -0.089	kg/s/m
	$q_{t,cross}$= 0.114	kg/s/m
N=1	$q_{b,cross}$= 0.155	kg/s/m
	$q_{s,cross}$= -0.124	kg/s/m
	$q_{t,cross}$= 0.031	kg/s/m;

using N=7 yields a larger bed-load transport (about 30%),but a smaller suspended transport (about 30%);
due to the opposite sign of the cross-shore bed load and suspended transport, small differences in each of these terms may result in a rather large difference of the total cross-shore transport (almost factor 4!);
the offshore transport at the bar crest is only weakly affected by the number of sand fractions (N=7 yields smaller transport rates because of the dominant influence of the suspended transport at the crest);
the sand transport gradients do not seem to be much affected by the number of size fractions.

Computational results for d_{50}= 0.0004 m and d_{50}= 0.0008 m showed similar effects.

4. SENSITIVITY COMPUTATIONS BED COMPOSITION AND BED LEVEL CHANGES; Test case symmetrical bar

To study the effect of selective transport proceses on cross-shore bed composition and bed level changes, a test case with low waves over a symmetrical bar is considered (see Figure 6). The toe of the bar is situated at -20 m and the crest of the bar at -3 m (below MSL). The bar slopes are 1 to 20. As the depth at both ends of the bar is relatively large (h= 20 m), the sand transport rate is zero under the present conditions with low waves. Hence, no sediment can enter or leave the computational domain. Sediment of a certain size fraction can only leave or enter the mixing layer via the base of this layer. The input data are, as follows:
$H_{1/3,0}$= 1 m, h_0= 20 m, θ= 20°, v_0 = 0 m/s, T_p= 8 s, $k_{s,c}$= 0.05 m, $k_{s,w}$= 0.05 m, γ= 0.7, d_{50}= 0.2 mm and N=4 (d_i = 0.1; 0.2; 0.3; 0.5 mm), (p_i= 0.2; 0.3; 0.3; 0.2).
Computed results after 1 month for various values of the mixing layer thickness (DL=0.05 to 0.25 m) and the hiding factor (h.f.=variable and 1) are given in Figures 6 and 7. The initial bed composition is uniform along the profile (d_{50}=0.2 mm). Deep water (offshore) is situated at x=0.
The most important results based on N=4 fractions are:
Effect of mixing layer thickness

- seaward of x=375 m the median particle size d_{50} decreases for all values of the mixing layer thickness DL, because the coarser particles are transported onshore in larger quantities than the finer particles (bed load transport is dominant);

- landward of x=375 m the median particle size d_{50} increases for all values of DL, because the coarser particles are deposited in this zone; furthermore coarser material is lost to the subsoil in the deposition zone;
- the effect of selective transport processes on the particle size distribution decreases with increasing value of DL;
- the bar crest migrates onshore for all values of DL (Figure 7); the migration rate of the crest is smallest for DL=0.05 m;
- the computed bed level after 1 month (Figure 7) is not much affected for DL between 0.1 and 0.25 m;
- the model yields stable results for all values of DL, provided that the time step is sufficiently small; DL=0.05 m requires a relatively small time step;

Effect of hiding factor

- the hiding factor was set to 1 for DL=0.15 m leading to a significant decrease of the fining process seaward of x=375 m (in the crest zone);
- a hiding factor of 1 leads to a reduction of the migration rate of the crest, which is caused by the increase (factor 2) of the offshore-directed suspended transport.

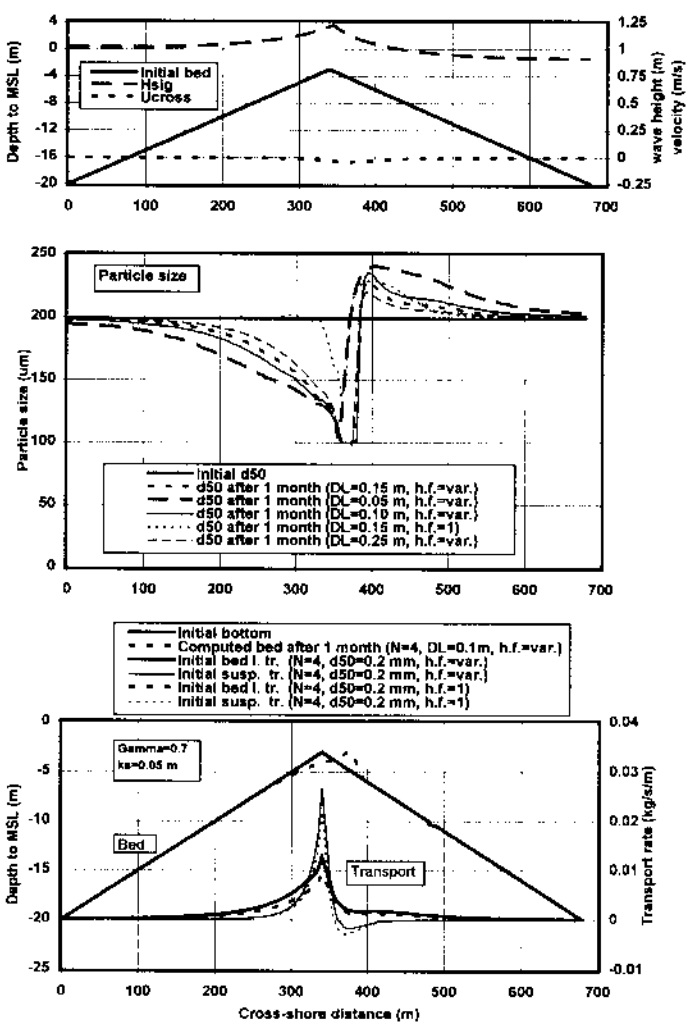

Figure 6 *Effect of mixing layer and hiding factor on computed bed composition and bed profile along symmetrical bar*

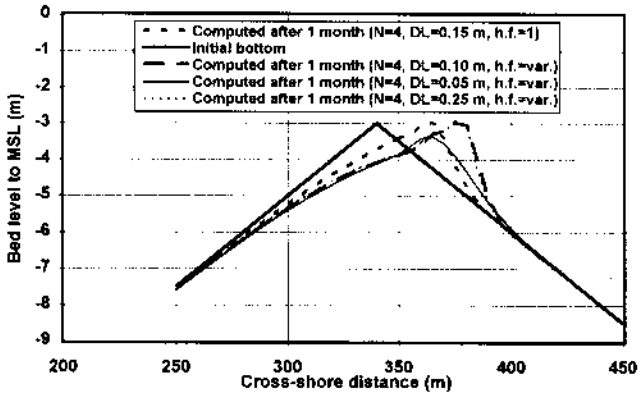

Figure 7 *Effect of mixing layer and hiding factor on computed bed profiles along symmetrical bar*

REFERENCES

Egiazaroff, P.I., 1965. *Calculation of non-uniform sediment concentrations, Journal of the Hydraulics Division, ASCE, Vol. 91, HY 4*

Hirano, M., 1971. *River bed degradation with armouring. Trans. JSCE, Vol. 3, part 2*

Houwman, K.T. and Ruessink, G., 1996. *Cross-shore sediment transport mechanisms in the surf zone. ICCE, Orlando, USA*

Kroon, A., 1994. *Sediment transport and morphodynamics of the beach and nearshore zone near Egmond, The Netherlands. Doc. Thesis, Dept. of Physical Geography, Univ. of Utrecht, The Netherlands*

Ribberink, J.S., 1987. *Mathematical modelling of one-dimensional morphological changes in rivers with non-uniform sediment. Dissertation, Civil Eng. Dep., Delft Univ. of Technology, Delft, The Netherlands*

Van Rijn, L.C., 1993. *Principles of sediment transport in rivers, estuaries and coastal seas. Aqua Publications, Amsterdam, The Netherlands*

Van Rijn, L.C., 1997. *Cross-shore modelling of graded sediments. Delft Hydraulics, Report Z2181, Delft, The Netherlands*

Van Rijn, L.C. and Kroon, A., 1992. *Sediment transport by current and waves, p.2613-2628. 23rd ICCE, Venice, Italy*

Van Rijn, L.C. and Wijnberg, K.M., 1996. *One-dimensional modelling of individual waves and wave-induced longshore curents in the surf zone. Coastal Engineering, Vol. 28, p. 121-145*

Wolf, F., 1997. *Morphology of bars in inner surf zone near Egmond, The Netherlands.Dept. of Physical Geography, Univ. of Utrecht, The Netherlands*